JOURNAL OF MATERIALS SCIENCE 29 (1994) 6167–6174

Hot workability of an Al–Mg alloy AA5182 with 1 wt % Cu

S. MARTINEZ DE LA PUENTE, B. VERLINDEN, L. DELAEY
Katholieke Universiteit Leuven, Department of Metallurgy and Materials Engineering, de Croylaan 2, 3001 Leuven, Belgium

A comparative study of the hot workability of two aluminium alloys, alloy AA5182 used for automotive applications and a variant modified with 1 wt % copper, has been carried out. Hot torsion tests were performed on both alloys subjected to two different heat treatments: a low temperature preheat to 450 °C and a high temperature preheat at 540 °C. The results from the torsion experiments are interpreted in terms of microstructural features. Both treatments produce the same strength, but the high temperature preheat leads to better ductility. This improvement is related to the homogenization of solute elements in the matrix; and, concerning AA5182 + Cu, also to the dissolution of a non-equilibrium Al–Mg–Cu ternary eutectic present in the as-cast microstructure. The precipitation of (Fe, Mn)Al_6 precipitates in the matrix of both alloys is induced by the high temperature heat treatment. Comparison of the results obtained by hot torsion shows that at low deformation rates AA5182 + Cu has better ductility than the classical alloy, but its ductility is lower at strain rates above 0.6–0.8 s^{-1}. The null ductility transition temperature is lower compared with that in the classical alloy, restricting the range of hot working temperatures. Inside this range the strength of both alloys is approximately the same, although the strain rate sensitivity coefficient is increased by copper additions. The experimental strength values follow the classical sinus-hyperbolic constitutive equation for hot working.

1. Introduction

An actual trend in the car industry is the substitution of steel for automotive body panels by lighter materials. This makes the cars less heavy and reduces the fuel consumption. It is required to find a material that is strong enough and has good formability. The main candidates are aluminium alloys, polymer matrix composites and "sandwich" structures of aluminium and polymers. Although the mechanical properties of aluminium alloys are inferior to those of steel, their lower density (three times lower than that of steel) leads to an improved specific strength (strength–weight ratio). This allows the use of thinner panels strong enough for automotive applications and leads to a considerable reduction in the weight of the car. In addition, the good corrosion resistance of aluminium alloys is another advantage with respect to steel. Among the classical aluminium alloys, Al–Mg alloys of the 5000 series, such as AA5182 and AA5052 in their fully annealed, O temper, condition, have been used for car body sheet applications because of their good combination of strength, corrosion resistance and formability. Lüders bands, however, may be formed in these alloys and restrict their use to inner car parts. The most severe Lüders bands or stretcher strain marks are a consequence of high yield point elongation, especially in fine grained alloys. Stretcher strain free material can be obtained by cold working slightly after annealing at the expense of a reduction in formability, or by a careful combination of cold deformation and annealing, which is economically disadvantageous. Age hardenable Al–Cu alloys (2000 series) and Al–Mg–Si alloys (6000 series) were also proposed [1, 2]. They are in general stronger but they suffer from reduced biaxial deformability, and a gradual reduction in their formability due to age hardening during storage may be a problem. A recent developement is the use of AA5182 modified with Cu [3]. It is claimed that the addition of Cu reduces the tendency for Lüders bands and has the additional advantage that the alloy becomes age hardenable. Age hardenability preferably during the painting cycle, i.e. *baking*, of the car would lead to an increased strength. This permits the use of thinner panels leading to lighter cars. Industrial rolling experiments however, have shown that an AA5182 alloy modified with 9 wt % Cu suffered from a poor hot deformability.

In the present work, a comparative study of the hot workability of an AA5182 alloy and a variant modified with 1 wt % Cu has been carried out by hot torsion simulations combined with microstructural investigations. The aim of this study is to clarify the influence of the initial microstructure present before deformation on hot strength and formability. It is required to understand the effect of copper addition on microstructural evolution during different heat treatments, and the influence of the developed microstructure on the mechanical properties of the alloy.

0022–2461

2. Experimental procedure

Microstructural analysis and hot torsion tests have been carried out on two types of alloys supplied in the form of direct cast ingots by Hoogovens Aluminium, Belgium. The compositions are mentioned in Table I. The first alloy is a classical Al–Mg alloy of type AA5182 and the second is a similar alloy modified with 1 wt % Cu. These materials have been studied in the as-cast condition and after two different homogenization treatments:

1. a continuous (logarithmic) heating up to 450 °C for 9 h followed by water quenching, referred to as "treatment L"; and
2. a continuous (logarithmic) heating up to 540 °C for 9 h followed by homogenization for 6 h at 540 °C and controlled cooling at 30 °C h^{-1} to 450 °C and finally water quenching, referred to as "treatment H".

The water quenching was carried out in a solution of H_2O + 5 vol%KOH + 5 vol%NaCl. Afterwards the samples were stored in liquid nitrogen until the start of further tests. Treatment H was chosen as a possible industrial homogenization scheme, with 450 °C as the starting temperature for hot rolling. Treatment L was chosen to study the influence of an incomplete homogenization. Hot torsion samples with a gauge radius of 4.5 mm and a gauge length of 24 mm were machined with their axes parallel to the casting direction. Hot torsion tests were carried out on a computer controlled hot torsion machine with induction heating, described elsewhere [4]. The specimens were placed in the torsion machine, heated at 50 °C s^{-1} to the test temperature and equilibrated for 3 min. During the equilibration time, one of the extremes of the torsion samples was left free to allow for thermal expansion during heating. Before starting the deformation the free end was fixed so that the length of the specimen remained constant during deformation. Torsion tests were carried out at 420, 450, 480 and 510 °C, and occasionally at higher temperatures. The true (surface) strain rates were 0.05, 0.2 and 1 s^{-1}. Samples were examined by light optical microscopy (LOM) and electron scanning microscopy (SEM). Microstructural analyses have been carried out with a Jeol 733 superprobe operating at 20 kV and equipped with both energy dispersive (EDS) and wavelength dispersive (WDS) analyses. Specimen preparation of aluminium alloys for microscopy is described in detail in [5].

2.1. Hot torsion test

A selection of torque–twist curves obtained at different temperatures and strain rates is shown in Fig. 1. In general the torque rises very quickly to a maximum and decreases gradually with increasing deformation. Fracture occurs before a real steady state is reached. The torque–twist curves (M, θ) have been converted into true stress–true strain curves (σ, ε) using the following formulae

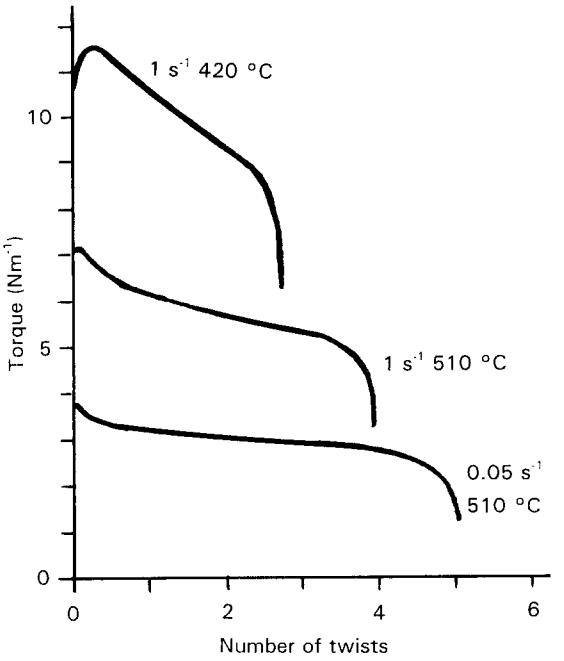

Figure 1 Torque–twist curves obtained at different deformation temperatures and strain rates for alloy AA5182 after pretreatment H.

$$\sigma = \frac{M3^{1/2}}{2\pi R^3}(3 + m + p) \quad \text{and} \quad \varepsilon = \frac{R\theta}{L3^{1/2}} \tag{1}$$

$$m = \left(\frac{\partial \log M}{\partial \log \dot{\varepsilon}}\right)_{T,\varepsilon} \quad \text{and} \quad p = \left(\frac{\partial \log M}{\partial \log \varepsilon}\right)_{T,\dot{\varepsilon}}$$

with R the gauge radius, L the gauge length, m the strain rate sensitivity coefficient and p the strain hardening coefficient.

Some values of the strain rate sensitivity coefficient, m, are given in Fig. 2. For both alloys m increases with increasing test temperature and decreases with increasing strain. For peak stress, the Cu bearing alloy has a higher strain rate sensitivity than the classical AA5182 alloy, but this difference levels out with increasing deformation.

The peak stress values of the two alloys after two different heat treatments (L and H) have been plotted in Fig. 3 as function of test temperature. It appeared that the addition of 1 wt % Cu to alloy AA5182 increased the peak strength slightly at lower test temperatures. As mentioned before it also increases the strain rate sensitivity of the peak stress. No significant difference in the peak strength could be observed between the high temperature and the low temperature homogenization treatments. The coefficients of the classical constitutive equation

$$\dot{\varepsilon} = A(\sinh \alpha\sigma)^n \exp(-Q/RT) \tag{2}$$

TABLE I Composition of the two alloys

Alloy (wt %)	Al	Mg	Mn	Fe	Si	Cu	Cr
AA5182	94.590	4.438	0.335	0.367	0.146	0.021	0.051
AA5182 + Cu	93.570	4.331	0.306	0.338	0.134	1.223	0.029

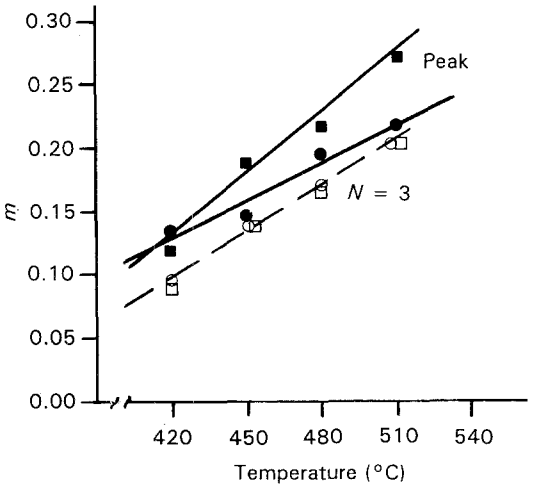

Figure 2 Strain rate sensitivity coefficient, m, as a function of the test temperature for two alloys after preheat H at peak deformation ($\varepsilon \sim 0.1$) and at three rounds ($\varepsilon = 2.04$): (○, ●) AA5182, (□, ■) AA5182 + Cu.

with Q the apparent activation energy, R the gas constant, T the temperature (in K) and A, α and n temperature independent constants, have been determined for the peak stress values and for the stress values after deformation of one round ($\varepsilon = 0.68$) and three rounds ($\varepsilon = 2.04$), respectively. Table II shows that the apparent activation energy, Q, of alloy AA5182 remains constant with increasing strain and has a value of 175 kJ mol^{-1}. The n coefficient increases with strain reflecting the decrease in strain rate sensitivity. The addition of 1 wt % Cu to the alloy increases the apparent activation energy to 180–190 kJ mol^{-1}. The increase of n with strain is higher than in the alloy without Cu. Fig. 3 shows the good correlation between the constitutive Equation 2 and the experimental data points for the peak stress.

Fracture strains, ε_f, as function of the test temperature have been plotted in Fig. 4. In general, the ductility is more or less constant over a certain temperature range and then it decreases abruptly towards zero. The addition of Cu has shifted the null ductility temperature towards lower values. The difference is higher after a low temperature homogenization treatment (L) than after a high temperature treatment (H). If for each alloy and strain rate an average ductility value is calculated over the different temperatures (with exception of the null or near-null ductility data) some other trends become apparent (Table III and Fig. 5) :

1. In all cases the ductility decreases with increasing strain rate.

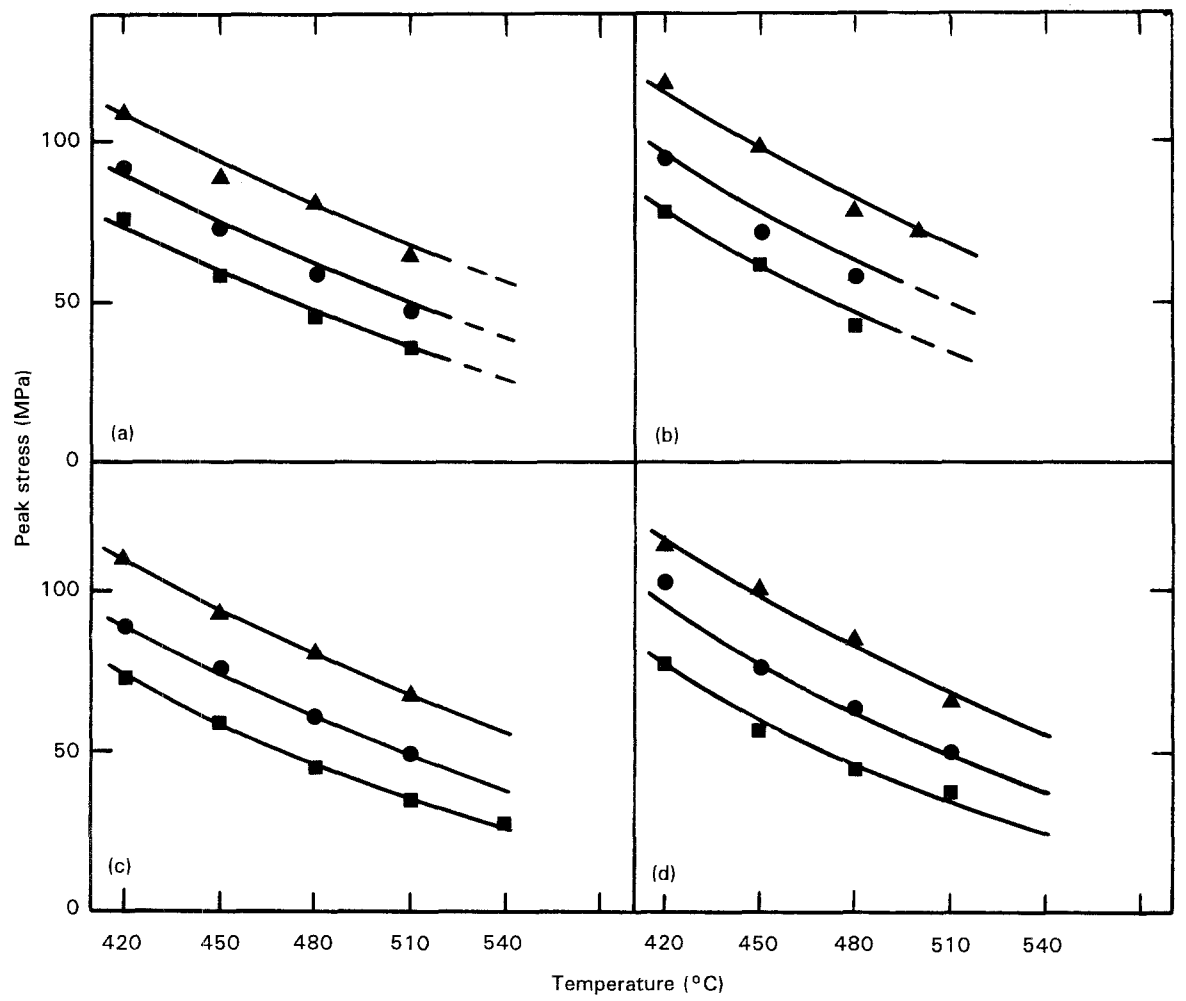

Figure 3 Peak stress as a function of test temperature for two alloys and two different pretreatments: L (logarithmic heating to 450 °C in 9 h) for (a) AA5182 and (b) AA5182 + Cu, and H (logarithmic heating to 540 °C in 9 h, 6 h at 540 °C and cooling to 450 °C in 3 h) for (c) AA5182 and (d) AA5182 + Cu. Full lines are calculated following the constitutive equations in Table II. (▲) $\dot{\varepsilon} = 1\ s^{-1}$, (●) $\dot{\varepsilon} = 0.2\ s^{-1}$, (■) $\dot{\varepsilon} = 0.05\ s^{-1}$.

TABLE II Constitutive equation for the alloys AA5182 and AA5182 + Cu derived for peak stresses and flow stresses at one and three rounds, respectively

$\dot{\varepsilon} = A[\sin h(\alpha\sigma)]^n \exp(-Q/RT)$

Alloy	Deformation	$\alpha(MPa^{-1})$	$A(s^{-1})$	n	$Q(KJ\,mol^{-1})$
AA5182	Peak	0.030	0.12525E11	2.77	175
AA5182	$N = 1$	0.030	0.23224E11	2.84	174
AA5182	$N = 3$	0.030	0.19649E11	3.62	173
AA5182 + Cu	Peak	0.030	0.41300E11	2.56	182
AA5182 + Cu	$N = 1$	0.030	0.92541E13	2.72	184
AA5182 + Cu	$N = 3$	0.030	0.38045E12	3.70	193

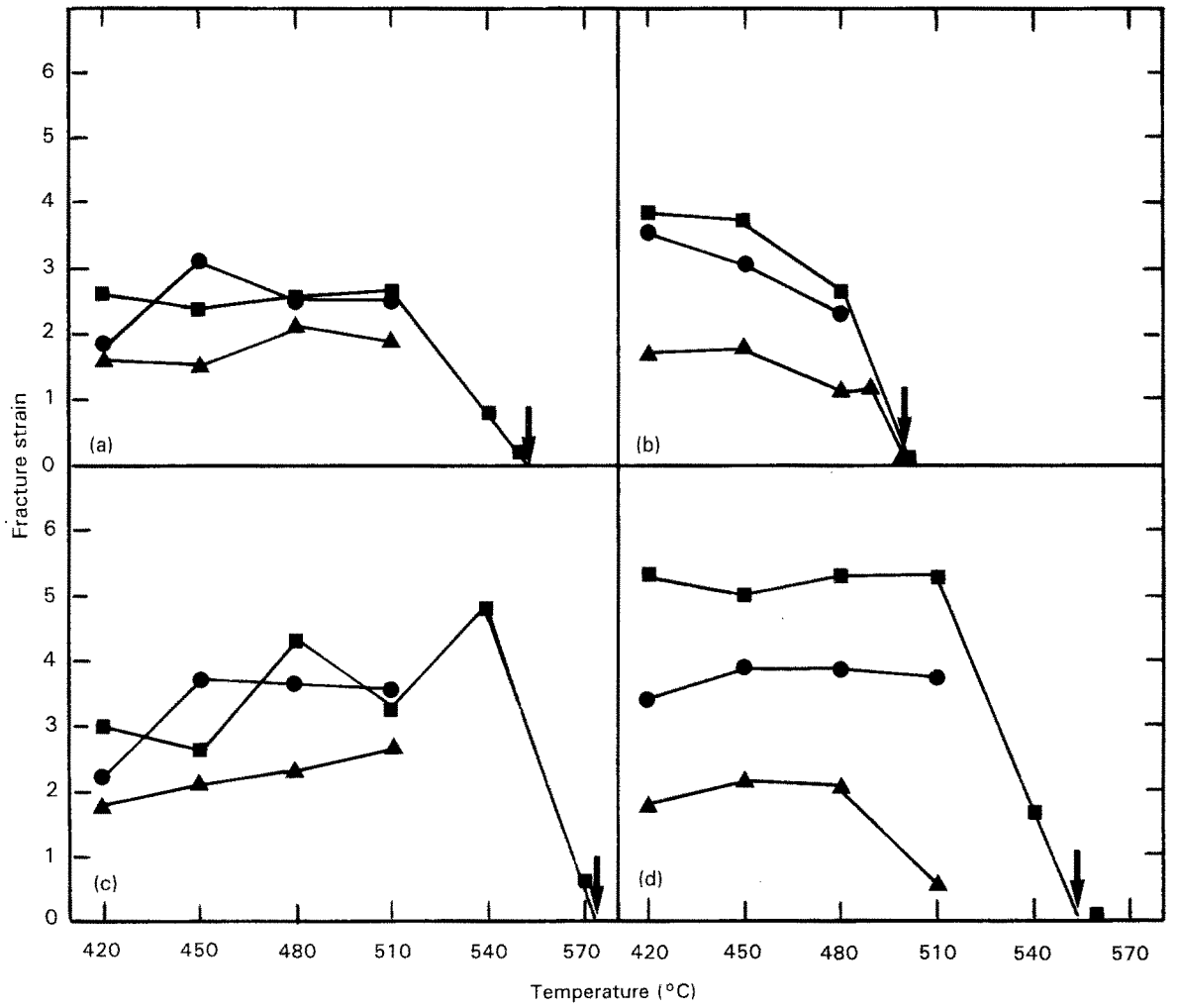

Figure 4 Fracture strain ε_f as a function of test temperature for two alloys and two different pretreatments. For treatment L: (a) AA5182 and (b) AA5182 + Cu. For H: (c) AA5182 and (d) AA5182 + Cu. (▲) $\dot{\varepsilon} = 1\,s^{-1}$, (●) $\dot{\varepsilon} = 0.2\,s^{-1}$, (■) $\dot{\varepsilon} = 0.05\,s^{-1}$, ↓ estimated null ductility temperature.

2. The ductility after treatment H is higher than after treatment L. The relative improvement is about 30%. Two exceptions are AA5182 + Cu at $0.05\,s^{-1}$ and 420 °C, in which the improvement is about 50%, and AA5182 at $1\,s^{-1}$ and 480 °C, with an improvement of about 20%.

3. The ductility of the Cu-modified alloy is much more sensitive to strain rate than that of the conventional alloy; at low strain rates the addition of Cu increases the fracture strain, but at higher strain rates (above 0.6–0.8 s^{-1}) it decreases the ductility.

Torsion tests carried out on as-cast samples have shown that the Cu-modified alloy was very brittle at present test temperatures and with alloy AA5182 only a very small deformation could be obtained prior to fracture.

2.2. Microstructural analysis

2.2.1. As-cast materials

The as-cast microstructure of both alloys consists of dendrites of aluminium with coarse interdendritic phases. In alloy AA5182 two kinds of constituents are found, both are shown in Fig. 6a: an Al–Mg–Si phase (dark) and an Al–Mn–Fe phase (light grey). The light

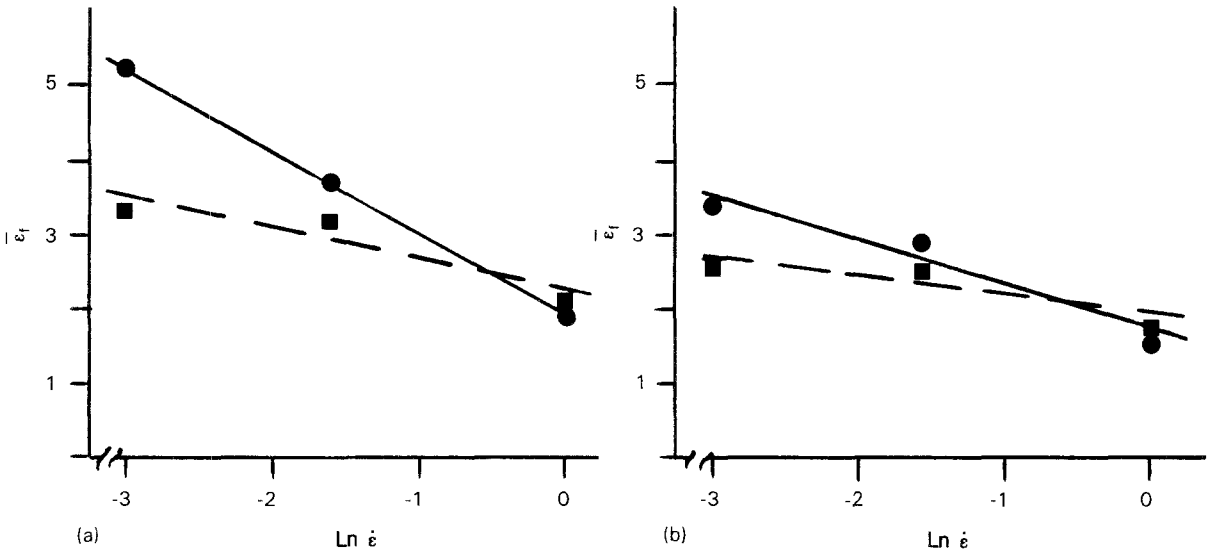

Figure 5 Average values of the fracture–strain at 420, 450 and 480 °C, as a function of strain rate: (a) for treatment H, and (b) for treatment L. (■) AA5182, (●) AA5182 + Cu.

TABLE III Average values of the strain to fracture at 420, 450 and 480 °C

Strain rate (s^{-1})	AA5182	AA5182 + Cu	Pretreatment
0.05	3.34	5.23	H
0.20	3.23	3.77	H
1.00	2.10	1.97	H
0.05	2.55	3.44	L
0.20	2.54	2.95	L
1.00	1.77	1.54	L

grey phase is most probably a fine mixture of Fe_3Al and (Fe, Mn)Al_6, as explained hereafter. It is well accepted [6] that the binary compound $MnAl_6$ can dissolve a considerable amount of Fe up to $Mn_{0.5}Fe_{0.5}Al_6$, which means Al ~ 86 at %, Mn ~ 7–14 at% and Fe ~ 0–7 at%. The solubility of Mn in $FeAl_3$ on the other hand is quite low. SEM–EDS point analysis of the light grey Al–Mn–Fe phase has shown the following composition: Al ~ 78–86 at%, Mn ~ 3–4.3 at% and Fe ~ 11–16.7 at%. The amount of Mn is too high for this constituent to be $FeAl_3$, and the Fe content is higher than

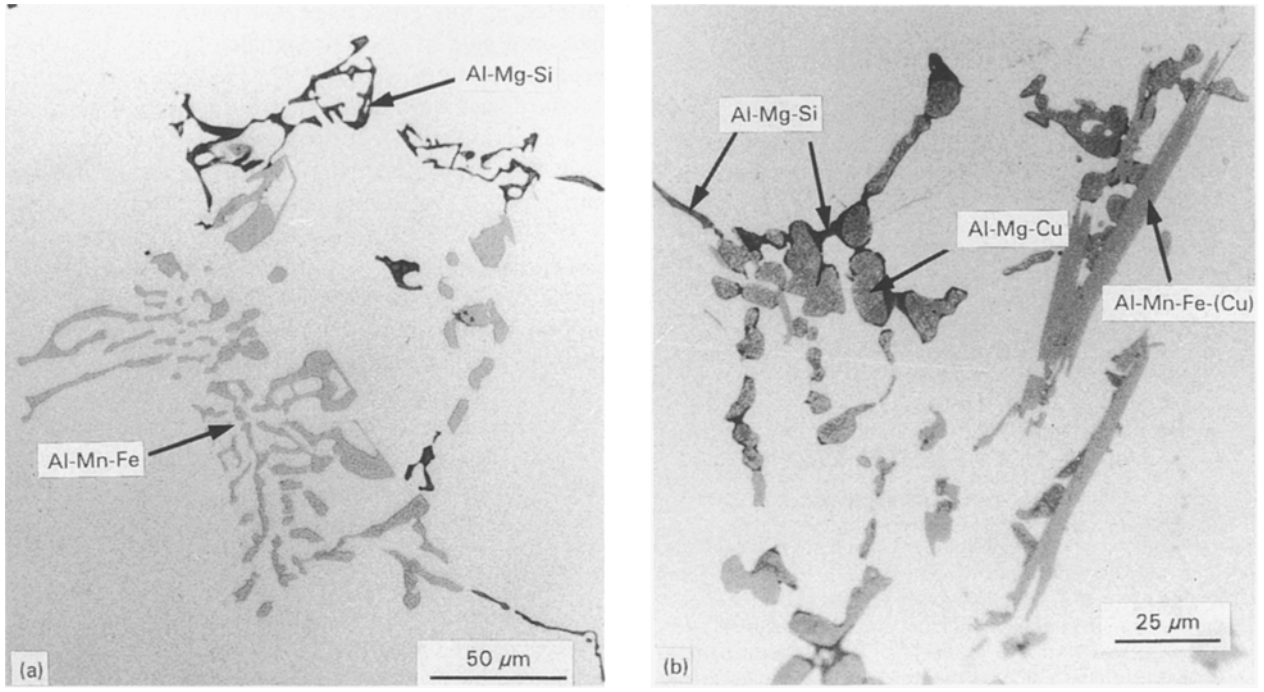

Figure 6 Coarse constituents found in the as-cast microstructure of both alloys: (a) AA5182 contains two kinds of constituents, both of irregular morphology; a dark phase containing Al–Mg–Si and a clear phase containing Al–Mn–Fe. (b) AA5182 + Cu as-cast contains a dark Al–Mg–Si phase, a light grey Al–Mn–Fe(+ Cu) phase of varied morphology, sometimes faceted, and a yellow (under LOM) Al–Mg–Cu phase, oval shaped and often arranged in chain-like structures along grain boundaries. Size variations of the constituent particles were observed in both alloys.

allowed by the $Mn_{0.5}Fe_{0.5}Al_6$ compound. This suggests that the light grey phase is a fine mixture of $FeAl_3$ and (Fe, Mn)Al_6 probably formed as a ternary eutectic during cooling from the melt. The Al–Mg–Si dark phase shows regions of different contrast in backscattered electron SEM images, indicating an heterogeneous composition. EDS analysis also registered compositional differences in these particles. In some points Si was more abundant than Mg, while in other regions the Mg content was slightly higher than that of Si. Since in other investigations [6] Mg_2Si particles were found as coarse constituents in the alloy AA5182, it is assumed that Mg_2Si is one of the compounds that makes up the heterogeneous dark constituent. Consideration of the Al–Mg–Si ternary phase diagram lead to the assumption that this phase could be a mixture of two eutectics; Al + Mg_2Si and Al + Mg_2Si + Si produced by non-equilibrium cooling. The alloy AA5182 + Cu contains three types of constituents, which are shown in Fig. 6b; the Al–Mg–Si and Al–Mn–Fe(+ Cu) particles also found in the classic alloy and an Al–Mg–Cu phase, yellow in LOM, oval shaped and sometimes forming chain-like structures. This phase is probably a low temperature melting eutectic of the Al–Mg–Cu ternary system.

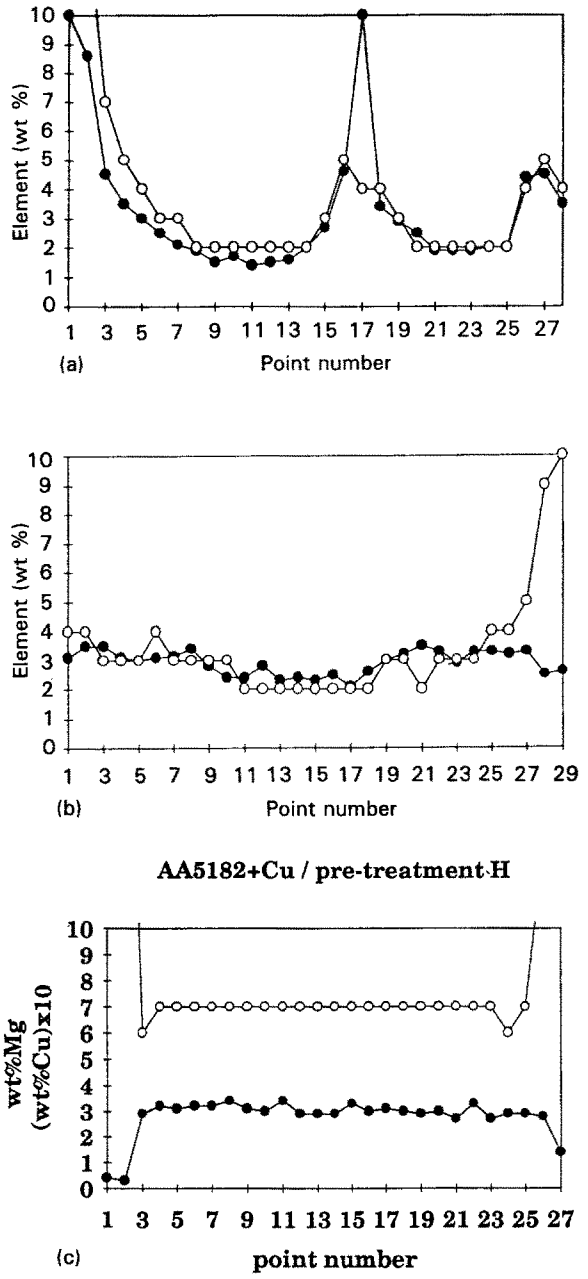

Figure 7 Line scans made on AA5182 + Cu in the as-cast condition and after the two pretreatments, showing the evolution of the distribution of Mg and Cu in the matrix: (a) AA5182 + Cu as-cast. There is segregation to grain boundaries and matrix–particle interfaces. The analysis starts on an Al–Mg–Cu constituent particle, continues through the interior of the grain, intersects an Al–Mg–Si particle at the grain boundary (at points ~ 15–18) and finishes in the next grain edge. (b) AA5182 + Cu, pretreatment L. The analysis starts in an Al–Mg–Si constituent and finishes in an Al–Mn–Fe constituent. (c) AA5182 + Cu, pretreatment H. The analysis starts and finishes in two Al–Mn–Fe particles. (●) Mg, (○) Cu (wt%) × 10.

The aluminium matrix of both alloys contained Mg as the major solute element. Small amounts of Mn and Fe were also found in solid solution (in amounts below 1 wt %), and in AA5182 + Cu, also copper was found. No Si was detected in solid solution, all of it being concentrated in the dark interdendritic particles. The distribution of Mg is highly inhomogeneous, with most of it concentrated near grain boundaries and at matrix–particle interfaces. The same consideration can be made about the copper distribution in AA5182 + Cu alloy. To illustrate this segregation line scans of Mg and Cu were performed in AA5182 + Cu as-cast alloys, and are shown in Fig. 7a. The line scans were made in steps of 8 μm to avoid interference between adjacent points. The analysis started in an Al–Mg–Cu particle located at a grain boundary. It continued across the grain and reached the edge intersecting an Al–Mg–Si particle, points 15–17. The next grain was also scanned with the analysis finishing in the grain boundary. No evidence of a constituent particle was detected at this grain edge. Cu concentrations were measured with WDS. The signals obtained by WDS were converted to K-ratio values using a pure copper standard, and were then converted to weight percentages applying a ZAF correction procedure. The ZAF correction procedure is an iterative technique usually employed for metals and alloys that corrects quantitative EDS/WDS data from atomic number effect (Z), absorption (A), and fluorescence (F). The ZAF correction factors used were the ones obtained by EDS for copper in aluminium. The relative error is of 1 wt %. Mg was analysed with EDS with a relative error of 5 wt %. In both grains the amount of Cu and Mg is seen to decrease towards the grain interior and to segregate to grain edges at matrix–particle interfaces and at grain boundaries.

2.2.2. Heat treated samples

The heat treatments L and H induce important changes in the microstructure. Treatment L produces the partial homogenization of Mg in both alloys and of Cu in AA5182 + Cu. No other microstructural feature is affected by heat treatment L. More changes take place during heat treatment H. In the matrix of both alloys complete homogenization of Mg and Cu is achieved, and the precipitation of small Al–Mn–Fe

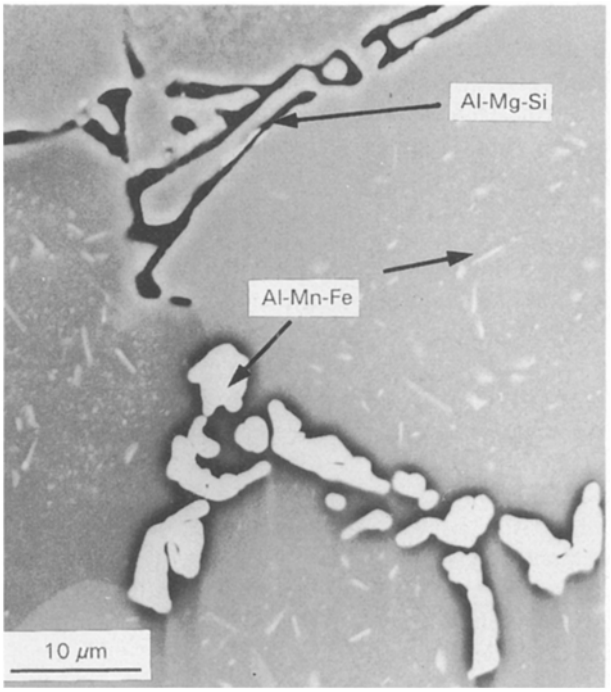

Figure 8 Al–Mn–Fe containing precipitates in AA5182. These precipitates were found in both alloys after pretreatment H. The precipitates have a needle and platelike morphology of approximately 5 μm length. Precipitate distribution is quite inhomogeneous.

dispersoids is induced. In Fig. 7b, c line scans performed in the heat treated samples of AA5182 + Cu alloy are shown to illustrate this homogenization process. In Fig. 8 matrix precipitates can be observed. These precipitates have a needle and platelike morphology (of approximately 5 μm length) and are very inhomogeneously distributed. They have been identified as (Fe, Mn)Al_6 precipitates [7], and the inhomogeneous distribution has been explained in terms of the segregation of Mn during solidification and the effect of Mg on the solid solubility of Mn [8, 9]. Another important event occurring in AA5182 + Cu during treatment H, is the dissolution in the matrix without melting of the Al–Mg–Cu phase. The Cu atoms of this constituent have gone to the matrix increasing the amount of Cu in solid solution as is evidenced by comparison of the line scans of Fig. 7. The Al–Mg–Si and Al–Mn–Fe intermetallics are not altered in any of the two alloys.

3. Discussion

The changes in hot strength and ductility induced by the different preheats will be correlated with the microstructural observations reported in the previous section.

3.1. Alloy AA5182

An increase in ductility is observed in the sequence as-cast–low temperature preheat L–high temperature preheat H. This can be explained in terms of homogenization of Mg in the matrix. Mg is a solid solution strengthening element that, when segregated to grain boundaries, leads to inhomogeneous deformation inside the grain and therefore, to lower ductility of the material. A more uniform distribution improves the ductility.

Treatment H leads to the precipitation of Al–Mn–Fe bearing dispersoids that have been identified as (Fe, Mn)Al_6. It is generally accepted that a fine distribution of second phase particles in the matrix will lead to some strengthening. On the other hand, a precipitation process supposes the release of supersaturation in the matrix, with a consequent loss in strength as the matrix becomes depleted of solutes. If the temperature increases, the dispersoids will redissolve leading again to solid solution strengthening and less second phase strengthening. In any case, both strengthening mechanisms, solid solution and dispersed second phase strengthening, loose efficiency as the working temperature is raised because the dislocations have more thermal activation to overcome the obstacles. In the present investigation, no significant differences in strength after L and H pretreatments are found, thus no appreciable change in high temperature strength of the alloy seems to be induced by this precipitation. Further work will be required to clarify the influence of these precipitates on the mechanisms of deformation.

The null ductility temperature of alloy AA5182 was found to occur around 570 °C in samples subjected to heat treatment H, while in samples subjected to heating schedule L it was around 550 °C. This shift to lower temperatures could be due to non-uniformity of the Mg distribution after the low temperature preheat. The matrix of samples that have not been totally homogenized contains regions of high Mg concentration with a melting point lower than the one predicted by the nominal alloy composition. This will lead to hot shortness when tested at deformation temperatures above the local melting point of these regions (it has to be remembered that the torsion samples have been water quenched after heat treatment and reheated to the test temperature in about 10–15 s). Fracture at 570 °C of samples subjected to treatment H, whose matrix has been completely homogenized, is supposed to be related to the Al–Mg–Si constituent. This conclusion is derived from observations of a sample heated up to 570 °C at 50 °C s^{-1} and fractured with no applied torque. It could be observed how the amount of dark constituent had decreased drastically, giving evidence of the instability of this phase at this temperature.

3.2. Alloy AA5182 + Cu

Similar considerations as those made for AA5182 are applicable for AA5182 + Cu alloy. Segregation of solutes to grain boundaries and matrix–particle interfaces impairs hot ductility. Complete matrix homogenization is achieved with treatment H, while some segregation still exists after the low temperature preheat L. This can explain some improvement in the ductility of the material after the H preheat. The (Fe, Mn)Al_6 precipitates apparently do not affect strength. The effect of these precipitates and the influence of the copper in solid solution on the hot ductility needs to be investigated.

Apart from those microstructural features mentioned above, the most observable microstructural difference with the classic alloy is the presence in the solidified microstructure of a coarse Al–Mg–Cu ternary phase. This phase exists as a coarse constituent in the as-cast condition, persists after treatment L and dissolves in the matrix without melting after H heat treatment. The improvement in ductility and shifts in null ductility temperature achieved with the heat treatments are assumed to be directly related to this microstructural change. The Al–Mg–Cu coarse constituent is considered to be a non-equilibrium ternary eutectic produced by non-equilibrium solidification that causes the failure of the material when suddenly heated in the torsion machine to a test temperature above the melting point of this non-equilibrium eutectic. When diffusion is allowed, as in slow heating during pretreatment, equilibrium is gradually restored and the non-equilibrium eutectic changes its composition towards the equilibrium one, increasing the local melting point and allowing for higher testing temperatures. After H heat treatment it dissolves into the matrix without melting, leading to a wider range of deformation temperatures.

4. Conclusions

A hot workability study of AA5182 and AA5182 + Cu alloys was carried out in order to clarify the influence of microstructure on the high temperature properties of both alloys. The following were concluded.

1. The as-cast microstructure of both alloys consists of dendrites of aluminium with coarse interdendritic phases. The coarse constituents in AA5182 have been identified as $FeAl_3$ + (Fe, Mn) Al_6, and a mixture of Al + Mg_2Si and Al + Mg_2Si + Si. In AA5182 + Cu the same constituents are found together with an Al–Mg–Cu phase that is assumed to be a non-equilibrium ternary eutectic. The Al–Mn–Fe constituent contains some copper as alloying element. The as-cast matrix of both materials presents appreciable segregation of Mg and Cu.

2. A preheat at 450 °C eliminates Mg and Cu segregation only partially. A high temperature preheat at 540 °C is required for complete homogenization of the matrix of both alloys. In addition, in AA5182 + Cu the Al–Mg–Cu constituent is dissolved. No changes in the other coarse constituents are induced by these preheats. Heating to 540 °C also induces the precipitation of (Fe, Mn) Al_6 dispersoids in the matrix of both alloys.

3. High temperature heat treatments improve the ductility of both alloys with respect to the as-cast condition. The best ductility was achieved with a preheat of 6 h at 540 °C. The improvements are related to the elimination of segregation in the matrix and, in AA5182 + Cu, also to the dissolution of the low melting Al–Mg–Cu eutectic. In the latter alloy, the dissolution of this phase allows higher deformation temperatures. The effect of (Fe, Mn)Al_6 precipitates on hot ductility needs to be investigated.

4. Comparison of the results obtained by hot torsion for both alloys shows that additions of copper to AA5182 alloy provides an improved ductility at low deformation rates, but decreases the ductility at strain rates above 0.6–0.8 s^{-1}. At normal hot rolling speeds the addition of Cu can thus complicate the industrial processing. It also restricts the range of hot working temperatures by shifting the null ductility temperature to lower values. Inside this range the strength is not significantly altered, although the strain rate sensitivity coefficient is increased.

Acknowledgements

This research was partly supported by the Belgian Ministry of Science Policy under UIAP contract No. 041. The authors wish to acknowledge Hoogovens Aluminium Belgium for supplying the as-cast material. One of the authors (S. Martinez de la Puente) wants to acknowledge the financial support of the Basq Government.

References

1. J. W. EVANCHO and J. G. KAUFMAN, *Aluminium* **53** (1977) 609.
2. K. CAMBELL, I. DOVERT, T. R. RAMACHANDRAAN and J. D. EMBURY, *Metals Forum* **2** (1979) 229.
3. T. KOMATSUBARA, T. MURAMATSU and M. MATSUO, European Patent No. 0259700B1, Bulletin 90/22, 1990 (Sky Aluminium Co., Tokyo (JP)).
4. B. VERLINDEN, *ATB Metallurgie* **29** (1989) 39.
5. "Aluminium Alloys" from Metals Handbook, 9th Edn, Vol. 9 revised by R. H. Stevens (American Society for Metals, Metals Park, OH, 1985) pp. 351–388.
6. P. VILLARS and L. D. CALVERT, "Pearson's Handbook of Crystallographic Data for Intermetallic Phases", Vol. 2, (American Society for Metals, Metals Park, OH, 1985) p. 1018.
7. P. A. HOLLINSHEAD, *Mater. Sci. Technol.* **8** (1992) 57.
8. T. H. SANDERS, *Metall.* **14** (1981) 177.
9. N. RAGHUNATAN and T. SHEPPARD, *Mater. Sci. Technol.* **5** (1989) 542.

Received 12 October 1993
and accepted 21 April 1994